Journal of the European Ceramic Society 22 (2002) 2155–2164
www.elsevier.com/locate/jeurceramsoc

Dispersions of micrometric powders of molybdenum and alumina in liquid paraffin: role of interfacial phenomena on bulk rheological properties

D.T. Beruto*, A. Ferrari, F. Barberis, M. Giordani

Dipartimento di Edilizia, Urbanistica e Ingegneria dei Materiali (DEUIM) Facoltà di Ingegneria, Piazzale J. F. Kennedy, Pad D, 16129 Genova, Italy

Received 19 October 2000; received in revised form 29 November 2001; accepted 28 December 2001

Abstract

The flow behavior of particles size about 10 μm of molybdenum and alumina powders in liquid paraffin at 20 °C has been evaluated under maximum shear rate D values of 100 (s^{-1}), 200 (s^{-1}) and 400 s^{-1}. The molybdenum suspensions slowly deviate from the Newtonian behavior while the alumina ones obey the Herschel–Bulkley model. The viscosities of the suspensions increase with the volume fraction (Φ) of dispersed solid phase. The molybdenum/paraffin system obeys the Einstein equation, while the alumina/paraffin one obeys the Krieger–Dougherty equation. The intrinsic viscosity of the molybdenum suspensions is about 10, while the one calculated for the alumina/paraffin dispersion is 5. The spreading data give an apparent surface diffusion coefficient equal to 5.1×10^{-3} mm^2 s^{-1} for the molybdenum/paraffin system, and equal to 2.6×10^{-2} mm^2 s^{-1} for the alumina/paraffin one. The average advancing dynamic contact angle for the molybdenum/paraffin system is equal to 26 and equal to 17 for the alumina/paraffin one. The interfacial data have been discussed on the background of a new theory on nanometric film and drops on non-equilibrium solid surfaces. The average potential of interaction between the solid surfaces and the liquid paraffin has turned out to be equal to $-60.9\times10^{-3}\pm10^{-2}$ J m^{-2} for molybdenum and $-62.6\times10^{-3}\pm10^{-2}$ J m^{-2} for the alumina one. The difference among the interfacial solid–liquid data can explain the observed differences between the bulk rheological properties of the 10 μm particle sized dispersions. The results allow us to expand to these kinds of dispersions the tailoring methods adopted for the ceramic colloidal dispersions. © 2002 Elsevier Science Ltd. All rights reserved.

Keywords: Al_2O_3, Mo; Paraffin; Rheology; Suspensions

1. Introduction

Much ceramic processing before firing requires an intimate degree of mixing between different kind of powders in order to produce dense bodies with high mechanical properties. The system formed by mixing alumina particles and molybdenum grains both in the micro and metric size range, has been proved to be a promising one for coupling high Young modulus with good toughness.[1–5] How to obtain a green body formed with alumina and molybdenum powders homogeneously mixed at the micro-scale is still a technological barrier that needs to be overcome. Dry mixing methods have failed in obtaining this goal, due to the great difference in the intermolecular and interparticle forces of the ceramic and the metal phases. Wet-processing methods are promising but they should be further explored. Because of the high difference in specific density between the metal and the ceramic phase and because of the oxidation properties of the metal, it is not so easy to choose a dispersing liquid medium where the metal particles do not react and do not settle during the mixing process. In a framework of a nationwide project on ceramic–metal composites,[6] we have obtained promising results[7] in mixing a suspension of about 10 μm Mo and Al_2O_3 particles in low viscosity liquid paraffin at 20 °C. However, any further progress in this area requires an advance in the knowledge of the flow behavior of this kind of suspension. For particles with at least one dimension in the range 10^{-3}–1 μm (colloids),

* Corresponding author. Tel.: +39-010-3536039; fax: +39-010-3536036.
E-mail address: dabe@unige.it (D.T. Beruto).

0955-2219/02/$ - see front matter © 2002 Elsevier Science Ltd. All rights reserved.
PII: S0955-2219(02)00004-3

dispersed in a liquid phase, it is well known that bulk macro scale viscosity is significantly related to solid–liquid interfacial properties.[8,9] Because of this the global rheological behavior of the suspension can be controlled through the solid–liquid interfacial forces, which does matter for surface diffusion, interfacial shear viscosity, interface solute adsorption and interfacial surface gradient.[8] Composition and microstructure of the dispersed solids are strongly related with the macro-flow behavior of the suspension, thus the control of these solid phase microstructures can be done by tailoring the solid/liquid interfacial transport phenomena.[10,11] It would be highly desirable to achieve the same results when the dispersed powders have an average dimension bigger than that corresponding to the colloidal particles. A distinguished feature of all colloidal systems is that the contact area between the particles and the dispersing medium is so large as to enhance the value of the total interfacial energy terms and of the related solid–liquid interfacial properties. When the dispersed particles are in the ten micrometers size range the value of the contact area is reduced from the one concerning the colloidal systems. However, the solid–liquid interfacial terms might still play a role, if the interfacial solid–liquid forces are so strong to compensate the reduction in the surface area value. Normal alkanes of general formula (CH_3–$(CH_2)_n$–CH_3) can have low viscosity and be liquid at temperature of 20 °C when n is in the range between 15 and 40.[13] The molecules develop a molar cohesive energy per (–CH_2–) group which is about 6.9 kJ mol^{-1}.[14] When these molecules are near to an oxide surface like alumina, and/or to a metal surface like molybdenum, they can be adsorbed on it, due to the action of strong and long distance van der Waals forces.[13,14] Thus, the interfacial properties of molybdenum/paraffin and of alumina/paraffin suspensions might have an influence on the correspondent flow behavior even when the dispersed particles are in the micrometer size range.

The experiments discussed in this paper have been designed to obtain data on the flow behavior of the paraffin suspensions, on the spreading rates of the paraffin on alumina and molybdenum substrates and on the corresponding paraffin dynamic contact angles. Whether or not the difference between the bulk viscosity values can be related with the difference between the interfacial solid/liquid properties is the item that will be discussed and illustrated in the following. A positive answer to this question might lead to new and inventive ways of adjusting processing parameters and particles dimension to enhance the degree of mixing between ceramic and metal powders at the micro-scale level. As far as we are aware, the systems alumina/paraffin and molybdenum/paraffin have not been extensively studied yet,[15] thus the data presented here can set the case for a closer observation on the nature of the interfacial phenomena with scanning polarization force microscopy (SPFM).[16]

2. Experimental

2.1. Materials

Two kinds of alumina powders were used throughout this work to form suspensions with liquid paraffin at 20 °C and at different volume fraction ($\Phi = v/v$) . The first set of samples (I–Al_2O_3) was characterized by a degree of purity equal to 99.8%. The grain were almost monosized with an equivalent spherical average dimension of about 7 μm in diameter. The second set of specimens (II–Al_2O_3) had a degree of purity equal to 99.7% and was formed by a mixture of grains in the sub micron and in the ten micron size range. Two kinds of high purity alumina plates 0.7 mm thick and 2D dimensions, respectively equal to 50×50 and 10×10 mm were used as the substrate for spreading measurements of the liquid paraffin and for dynamic contact angle analysis.

Molybdenum powders with a degree of purity equal to 99.5% were used to form a suspension with liquid paraffin. Molybdenum plates, 0.7 mm thick and planar dimension, respectively equal to the ones above reported for alumina were used for spreading and dynamic contact angle measurements.

Commercial liquid paraffin, as liquid phase at 20 °C, formed by a mixture of C_{15}–C_{40} alkanes with density of 0.850 g cm^{-3}, was used as the dispersing medium of the ceramic and of the metallic powders.

Acetone (99.8%), *n*-hexane (99%), *o*-xilene (99%) were used to clean the alumina and the molybdenum plates before any spreading and dynamic contact angle measurements.

3. Methods

3.1. Powders characterization

SEM observations up to ×10,000 were made on both ceramic and metallic powders. The image Pro Plus software program was used to elaborate the SEM pictures and to find the average grain size distribution. To establish whether or not the molybdenum powders were covered by a thin film of oxide, a sample of molybdenum powder was placed into a thermobalance and then it was heated up to 1100 °C at a heating rate of 10 °C min^{-1} in a 1 atm nitrogen environment with a flux of nitrogen and 3% of hydrogen. Weight loss has been continuously recorded.

3.2. Suspensions preparation and rheological measurements

Dispersion of alumina and molybdenum particles were directly prepared by mixing a weighted quantity of

the solid phases with liquid paraffin at 20 °C. The powders were placed in a beaker with the mixing liquid and stirred by a rotating magnetic stirrer at a rate of 200 min^{-1} and at 20 °C under vacuum. It has been observed that this procedure allowed us to get rid of the air entrapped among the particles and it improved the wettability between the liquid paraffin and the solid phase. A laboratory rheometer "Rotovisco RV 20" equipped with Searle system shear-controlled head M5 and a NV sensor in double vain geometry was used to evaluate the flow behavior of the suspensions. The space between the inner and the outer cylinder of the stator (cup), filled with the suspension, accepts the bell-shaped rotor as it can be seen in Fig. 1. Because of the low thickness between the wall of the sensor, about 0.35 mm, the profile of the tangential velocity inside the suspension is linear for each applied shear rate D. The temperature was set and controlled at 20 ± 0.1 °C. Calibration of the instruments has been done using the liquid paraffin ($\eta = 0.20$ Pas) as sample test. Taking into account all sources of experimental errors it has been observed that the scattering on the viscosity measurements was equal to $\pm10^{-2}$ Pas. Each suspension underwent four times to the following cycling: constant acceleration from 0 to the max D, symmetrical return to quiet; every step lasting 60 s. The D max value was fixed respectively equal to 400, 200 and 100 s^{-1}.

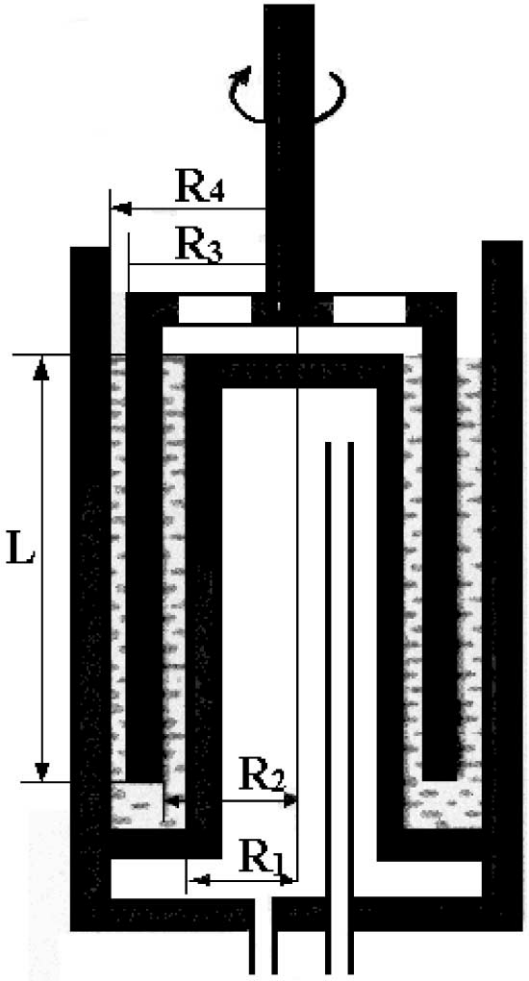

Fig. 1. Schematic representation of NV sensor in AISI 316 stainless steel: R1 = 17.5 mm, R2 = 17.85 mm, R3 = 20.1 mm, R4 = 20.5 mm, L = 60 mm.

3.3. Liquid paraffin spreading measurements

Alumina plates of $50\times50\times0.7$ mm were first immerged in a vessel containing *n*-hexane, for 20 min. Then the sample was taken out and placed in a second vessel with acetone for the same time. Finally it was dried and as soon as a possible it was used as a substrate for a liquid paraffin drop. Drops, whose volumes varied from 0.7 to 2 mm^3 were generated by a sterile syringe. The drops were placed on a substrate where a scale had been previously fixed to follow the spreading. Pictures were taken every 5 min. It was observed that within 60 min, the drops, independently from their initial volume, stopped spreading. The images of the drops were taken through a digital system of acquisition coupled with an optical microscope at ×6.5 magnification. The experiments were run at room temperature. Molybdenum plates were used in the same way but, for any spreading test, they were also cleaned with a mixture of xilene (50%) and of *n*-hexane (50%) before the normal hexane treatment.[17]

3.4. Dynamic contact angle measurements

The well-known Wilhelmy slide method[14] was used to measure the advancing and receding dynamic contact angle between liquid paraffin and the two metal and ceramic solid phases. Cleaned plates of alumina and molybdenum ($10\times10\times0.7$ mm) were hung from the wire of a microbalance and then immersed, at constant speed, into the liquid paraffin as illustrated in Fig. 2. After that the samples had reached a depth of 2–4 mm into the liquid phase, selected according to the speed, they were taken out at the same velocity. The in–out

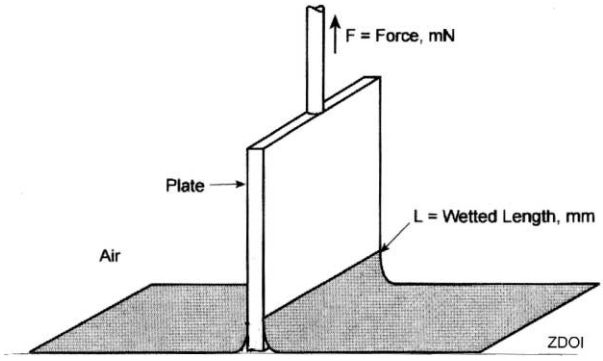

Fig. 2. Drawing of the plate just immersed into liquid paraffin, zero level ZDOI, in the dynamic contact angle analyzer.

loop was automatically performed and repeated on fresh and clean sample three time to test the reproducibility of the data. Six different velocities, ranging from 2 to 24 μm s^{-1}, were used in different loops to establish the dependence of the dynamic contact angles from the in–out speed. The resulting force acting on the sample was continuously recorded. The dynamic contact angles were evaluated from the value of the resulting force which reads:[18]

$$F^{T} = F - mg = P\gamma\cos\vartheta - \rho gV \quad (1)$$

At zero level (ZDOI) there is no immersed sample ($\rho gV = 0$) thus:

$$F^{T} = F - mg = P\gamma\cos\vartheta \quad (2)$$

where F^{T} is the total force measured by the instrument; m, P are, respectively, the mass, the immersed perimeter of the sample; ϑ is the contact angle and γ is the surface tension of the liquid. The sensitivity of the instruments is about $\pm 10^{-2}$ degrees for measurements of the contact angle and $\pm 10^{-4}$ mm as far as the stage travel is concerning. Experimental errors on the same samples tested under the same conditions have turned out equal to ±4% of the measured value. Calibration of the instrument was done by measuring the surface tension of water for chromatography (HPLC) with a plate glass. The measured value was 72.28 dyn cm^{-1}, very close indeed to the tabulated value of 72.75 dyn cm^{-1} for absolute pure water.[14] The surface tension of the liquid paraffin was consequently measured.

4. Results and discussions

Figs. 3 and 4 show, respectively, the typical microstructure of I–Al_20_3 and Mo particles that have been used as dispersed solid phase in liquid paraffin at different concentration (% in v/v). The I–Al_2O_3 particles (Fig. 3) have a block-like shape somewhat plate-like with a narrow size distribution. The grains are not porous and by assuming a spherical equivalent model with particles of about 7 μm in diameter, a specific surface area of 0.21 m^2 g^{-1} can be derived. The molybdenum powders (Fig. 4) are formed by round individual grains of about 2 μm which are joined through grain boundaries in clusters that can be estimated as 10 μm in size. The calculated value of the correspondent specific surface area is equal to 0.29 m^2 g^{-1}. On these grounds it can be argued that when these powders are dispersed in liquid paraffin at the same volumetric concentration, the solid–liquid interfacial area should be almost the same for both suspensions providing we neglect the solid–solid particle interactions.

Fig. 5 shows the typical flow curves τ vs. D, τ, being the applied shear stress (Pa) and D the shear rate (s^{-1}), for 10% Mo-dispersion (curve a), 10% I–Al_2O_3 dispersion (curve b), and liquid paraffin (curve c) at 20 °C. The liquid paraffin and the molybdenum suspensions show a linear behavior which is typical of Newtonian fluids. The corresponding viscosity for these kinds of

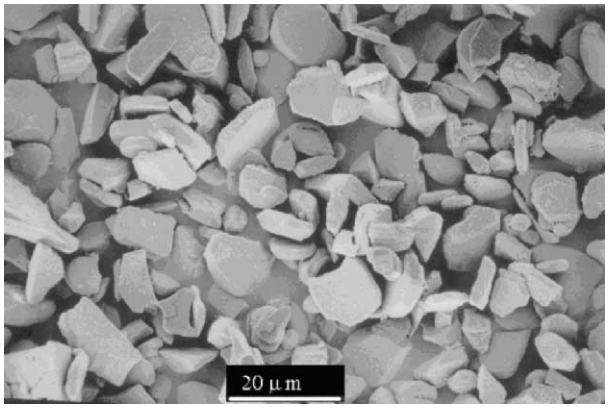

Fig. 3. Typical SEM picture of I–Al_3O_3 powder (1000×).

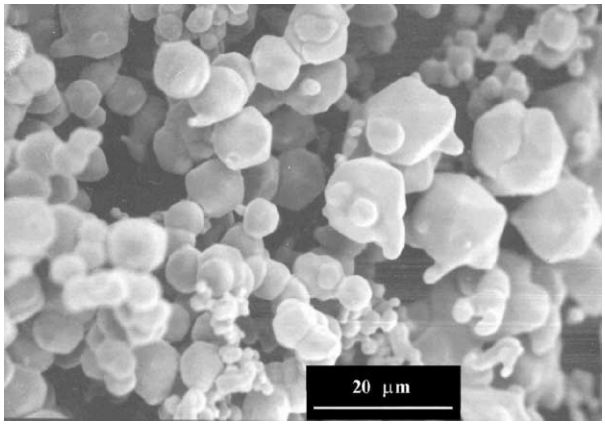

Fig. 4. Typical SEM picture of molybdenum powders (1000×).

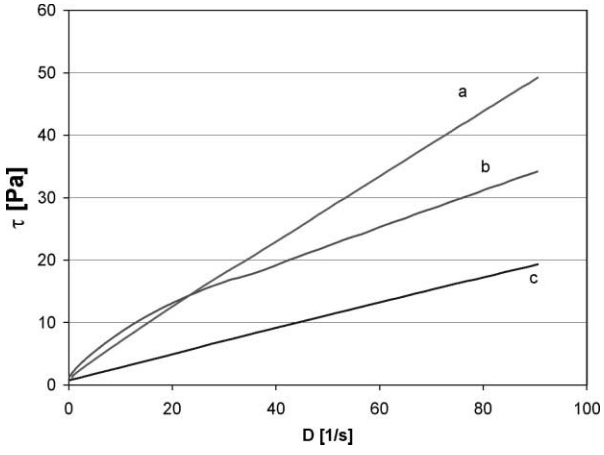

Fig. 5. Typical flow behavior for: (a) 10% molybdenum contaminated/paraffin suspension; (b) 10% I–Al_3O_3/paraffin suspension; (c) liquid paraffin; maximum applied shear rate $D = 100$ s^{-1}.

fluids are, respectively, equal to 0.20 Pas (liquid paraffin) and 0.6 Pas (molybdenum suspension). The flow behavior of the I–Al_2O_3 suspensions (curve b) obeys the Herschel–Bulkley model:[19]

$$\tau = \tau^{\circ} + \eta^* D^n \tag{3}$$

where η* is an apparent viscosity and n is a phenomenological coefficient. From the experimental data (see Fig. 5) the value of these parameters are $\eta^* = 0.3$ Pas and $n = 0.75$. No significant τ^0 has been observed when the volume fraction of the dispersed (I–Al_2O_3) powders is less than 0.15.

Fig. 6 (squares = I–Al_2O_3, circles = Mo) shows the dependence of the phenomenological coefficient n from the dispersed solid volumetric fraction (Φ). In agreement with the Newtonian behavior of the 10% molybdenum suspension (see Fig. 5) the corresponding value of n is very near to unity (0.96) and it does not change with the increase of the dispersed solid volumetric fraction. For the I–Al_2O_3 suspensions (squares, Fig. 6) the exponent n decreases as the concentration of the dispersed ceramic phase is increased between 0.02 and 0.20 (v/v). It has been observed that the ceramic-paraffin dispersions show a plastic behavior, with a yielding stress τ^0 greater than 5 Pa, when the I–Al_2O_3 powders volume fraction exceeds the value of 0.15. Accordingly the alumina particles dispersed in paraffin should have a tendency to aggregate at a higher concentration.[9] The tabulated Hamaker constants[13] for alumina and metal across water are respectively 3.67×10^{-20} J and $30–40\times10^{-20}$ J. If this difference holds also for liquid paraffin, the long range attractive van der Waals forces are greater between the Mo particles than between the Al_2O_3 ones. It is, therefore, surprising that Mo-suspensions do not show any yielding stress when the dispersed metal concentration increases. Very reasonably a thin layer of oxide covers the metal surface particles. Indeed weight loss measurements carried out on the molybdenum powders show that these powders, between 500 and 600 °C, lose the 1% of the initial weight when they are heated in a nitrogen environment with a flux of nitrogen with 3% of hydrogen. Assuming for the molybdenum oxides an average density of 5.58 g cm^{-3},[12] the thickness of the film of oxide on the molybdenum particles can be calculated to be in a range from 5 to 7 nm.

Fig. 7 shows the effect of the concentration of the dispersed solid phase on the apparent viscosity of the Mo (circles) and of the I–Al_2O_3 (square points) suspensions. In agreement with the expected predictions for suspensions that obey the Newton and the Herschel–Bulkley model,[9,20], the viscosity of the Mo dispersion and of the I–Al_2O_3 dispersion increases with the concentration of the solid dispersed phases. For the molybdenum suspensions, that slowly deviate from the Newton law, the effect of solids loading on its flow behavior is described by the well known Einstein relationship:

$$\eta = \eta_C(1 + \phi[\eta]) \tag{5}$$

where η is the intrinsic viscosity and η_C is the viscosity of the dispersing medium. For the alumina suspensions, the Krieger–Dougherty equation,[21] which reads:

$$\eta = \eta_C\left(1 - \frac{\phi}{\phi_M}\right)^{(-[\eta]\phi_M)} \tag{6}$$

where ϕ_M is the maximum volume fraction of the solid dispersed, can be used to fit the experimental data if the value of the intrinsic viscosity is known. When the dispersed solid volume fraction, Φ, is less than 0.05 the hydrodynamic and Brownian many-body interactions should not affect the rheological bulk behavior. In this dilute system regime the intrinsic viscosity[22] of the suspension is defined as:

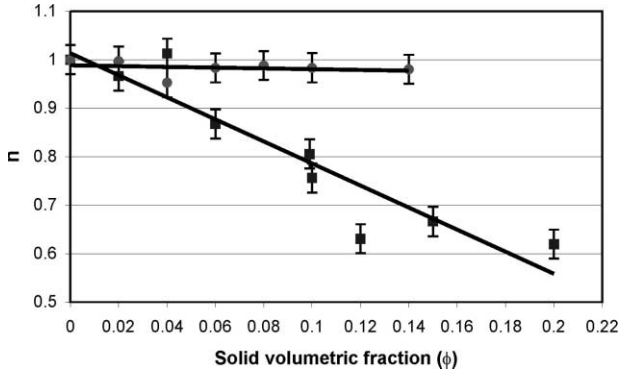

Fig. 6. Effect of the dispersed volume fraction on the value of phenomenological parameter n: circles = molybdenum contaminated/paraffin system, squares = I–Al_2O_3/paraffin system; linear regression are marked for both systems.

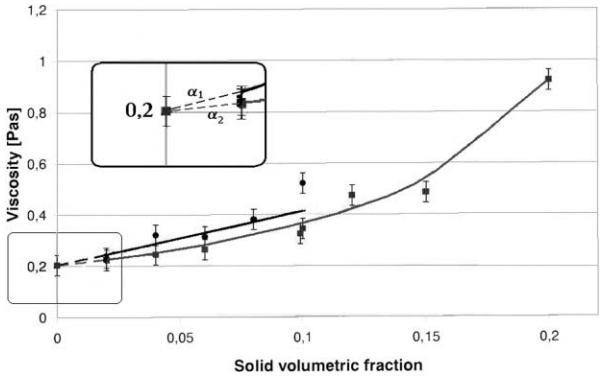

Fig. 7. Effect of the dispersed solid volumetric fraction on the viscosity of the suspensions: circles = Molybdenum contaminated/paraffin suspensions, squares = I–Al_2O_3/paraffin dispersed solid volumetric fraction; curve a: Einstein linear regression; curve b: Krieger–Dougherty regression; α_1 = initial slope for molybdenum contaminated/paraffin system, α_2 = initial slope for I–Al_2O_3/paraffin system.

$$[\eta] = \lim_{\Phi \to 0} \left[\frac{\frac{\eta}{\eta_C} - 1}{\Phi} \right] = \lim_{\Phi \to 0} \frac{\frac{\partial \eta}{\partial \Phi}}{\eta_c} \quad (4)$$

with the above mentioned symbolic notation. The intrinsic viscosity should be equal to 2.5, if the particles are hard-spheres and if the dispersing medium is Newtonian.[22] From the value of the initial slope α_1 and α_2 (see detail in Fig. 7), the intrinsic viscosity has been calculated equal to 10.24 for Mo-paraffin suspensions, and equal to 4.9 for the I–Al_2O_3/paraffin one. Both values are greater than Einstein's prediction. As it has been observed[20] this may be due to the effect of particle shape; however, the observed difference may also be related to the differences in interfacial viscosity between the ceramic and the metal paraffin dispersion.[8] On the grounds of these results the Krieger–Dougherty model fits the I–Al_2O_3 experimental data when Φ_M is equal to 0.33.

Figs. 8 and 9 describe typical overviews of two drops of liquid paraffin spreading, in air, over substrates of molybdenum (Fig. 8) and of alumina (Fig. 9). The radii of the drops (R_i), measured at the solid/liquid interface level (see Experimental section), are changing with time accordingly to a kinetic illustrated in Fig. 10. The radius dynamic is closely fitted by a diffusive like law:

$$R_i \propto D^{\frac{1}{2}} \cdot t^{\frac{1}{2}} \quad (7)$$

for a period included between 1 and 45 min. Visual observations indicate that the drops spontaneously stop to spread on both substrates after about an hour. The shape of the drops on the Mo substrate is characterized by a finite contact angle value at the solid/liquid interface level for all the spreading period. The value of the contact angle has been measured near to 15° at the end of the spreading step. By comparison with these data, the shape of the drops on the alumina substrate seems to be characterized by a lower topographic height and by a final contact angle value near to zero. Evidently the drop of liquid paraffin tends to spread as a liquid film on the alumina substrates, while it tends to stand as a drop on the molybdenum one. The coefficient D has been evaluated to be equal to 2.6×10^{-2} mm^2 s^{-1} for the Al_2O_3/paraffin interface and equal to 5.1×10^{-3} mm^2 s^{-1} for the Mo/paraffin one. Taking into account that for metals like Mo the freshly cleaved surfaces are readily contaminated in air,[23] and considering the experimental results obtained by heating the molybdenum powders in nitrogen flux, we can reasonably argue that a thin film of molybdenum oxide is also located on the Mo-plates which have been exposed to the air. If the Mo-surface would be formed by freshly cleaved metal, the liquid paraffin would spread on it at a higher rate because of the value of the metal Hamaker constant.[13] Since this evidence has not been observed, the metal surface has to be contaminated. From here on let us to call the Mo-plates tested in air and/or in the paraffin environment as Mo-contaminated samples. Viscous flows are acting at the solid/liquid interface during the spreading of the paraffin drops on different substrates. Thus the surface diffusion coefficients are inversely related with the paraffin surface viscosity. Accordingly the paraffin surface viscosity at the Mo-contaminated/paraffin interface is higher than the paraffin surface viscosity on the Al_2O_3 substrates. This result is in nice agreement with the observed difference between the intrinsic viscosity of the Mo and of the Al_2O_3 paraffin suspensions.

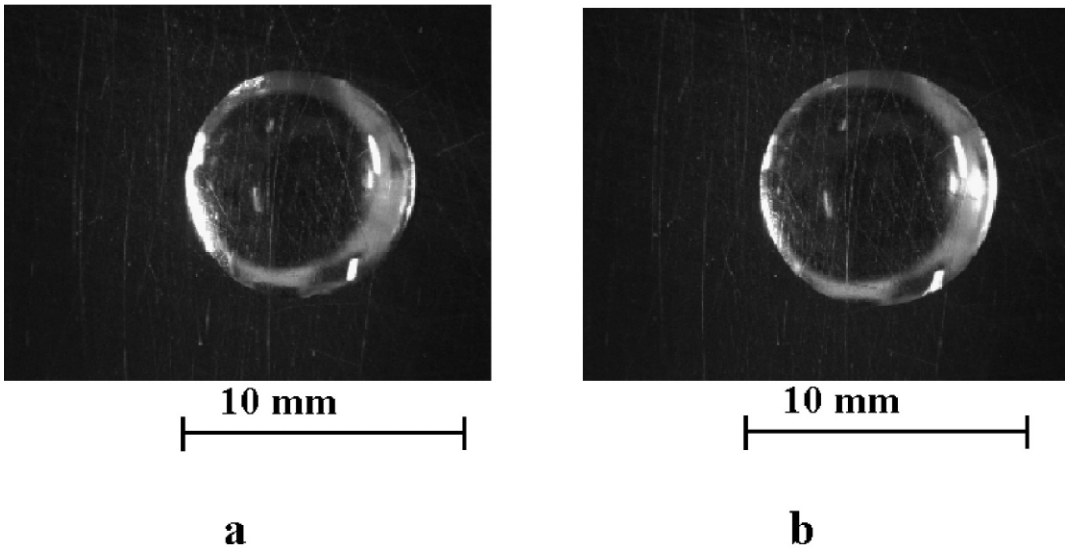

Fig. 8. Overview of liquid paraffin drop on molybdenum contaminated plate; (a) after a period of time equal to 5 min; (b) after a period of time equal to 45 min.

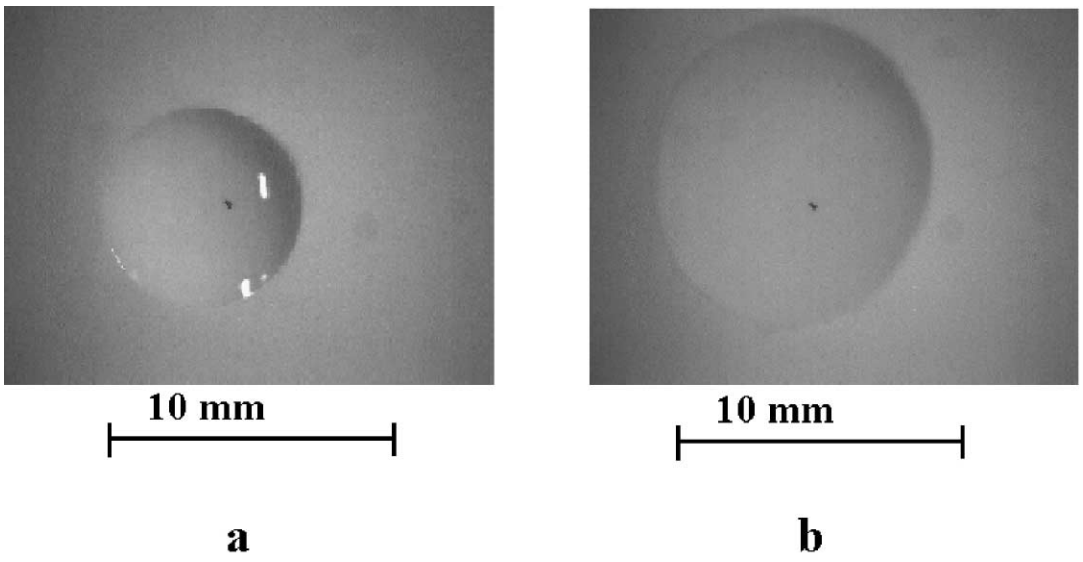

Fig. 9. Overview of liquid paraffin drop on alumina plate; (a) after a period of time equal to 5 min; (b) after a period of time equal to 45 min.

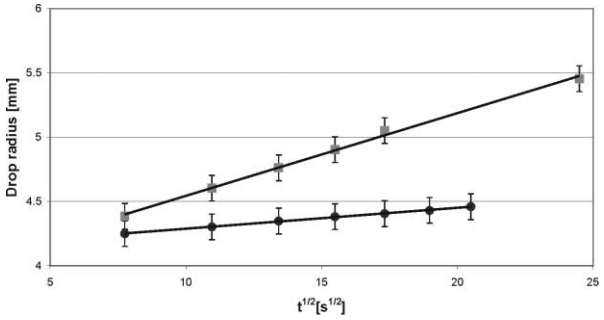

Fig. 10. Kinetic of spreading of liquid paraffin sessile drops on different substrates; square: on alumina plate; circles: on molybdenum contaminated plate.

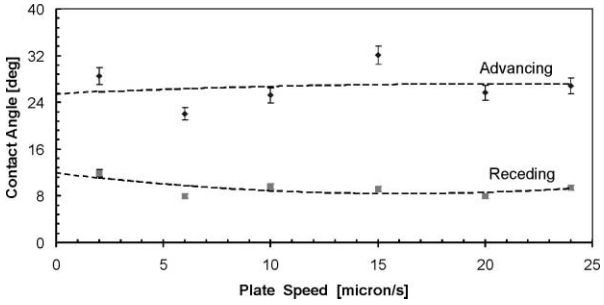

Fig. 11. Effect of the speed of immersion on dynamic contact angle measurements for molybdenum contaminated/paraffin system. Intercept of the dotted curves with vertical axis leads to static contact angle value.

Figs. 11 and 12 illustrate the values of the advancing and receding dynamic contact angles measured on the same Mo-contaminated/paraffin (Fig. 11) and Al_2O_3/paraffin (Fig. 12) systems with the Wilhelmy slide method.[14] Since the spreading of the paraffin over the metal and the ceramic substrates involves the flow of fluid over the solid, the contact angles also depend on the speed at which the solid slab advances or recedes into the paraffin. The value of the angles evaluated from:

$$\vartheta_i(0) = \lim_{v_i \to 0} \vartheta_i(v_i) \tag{8}$$

where ϑ_i is the advancing and/or the receding angle and v_i is the slab speed into the paraffin, is related with the static quantity that quite often[13,14] is used in describing the equilibrium and/or the quasi-state equilibrium between a liquid drop and/or film over a solid surface. By applying the Eq. (8) to the data of Figs. 11 and 12 the static contact angle values reported in Table 1 can be derived. It is possible to observe that both advancing

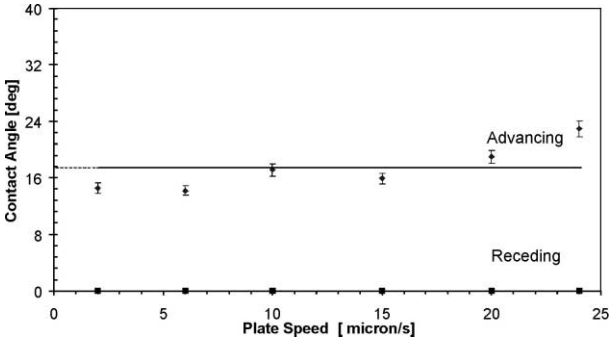

Fig. 12. Effect of the speed of immersion on dynamic contact angle measurements for alumina/paraffin system. Intercept of the dotted curves with vertical axis leads to static contact angle value.

and receding angles in the Mo-contaminated/paraffin system are always greater than the corresponding values in the Al_2O_3 /paraffin one. Furthermore for both systems the advancing angle is always greater than the receding one.

To understand these results a detailed thermodynamic analysis for nanoscale films and macroscopic drops on

Table 1
Alumina/paraffin and molybdenum/paraffin dynamic contact angles and calculated interaction energies

Samples	Static advancing angle (degrees) experimental error ±4%	Static receding angle (degrees) experimental error ±4%	Calculated interaction energy for advancing step λ (J m^{-2})	Calculated interaction energy for receding step λ (J m^{-2})
Alumina paraffin	17	0	-62.6×10^{-3}	-64.0×10^{-3}
Molybdenum paraffin	25	12	-60.9×10^{-3}	-63.3×10^{-3}

solid substrates is required. Here we summarize briefly the basic findings already published by Searcy,[24] which gives the key elements to discuss the above reported data. The Young–Dupre equation assumes that a drop takes a shape on a planar surface that minimizes the sum of the particle-vapor, substrate-vapor and particle-substrate integral interfacial free energy.[24] But quite often the substrates interfaces are thermodynamically unstable relative to roughening and to impurities. In this more realistic case, it is possible to work-out a model that allows us to derive the shape of the drop on the assumption that the partial free energy of the drop reaches a minimum value, but the partial free energy of the substrate may not. Accordingly, the value of the liquid/solid contact angle can be written as:[24]

$$\cos\vartheta = -\frac{(\gamma+\lambda)}{\gamma} \tag{9}$$

where γ is the surface tension of the liquid and λ is the average partial free energy of bonding of the liquid to the substrates. The quantity λ is dependent upon all repulsive and attractive forces acting from the first adsorbed layer to the last one before the bulk liquid phase. Its value, negative for all effective contact angles ranging between 0 and 90°, is an indication of the stability of molecules inside the solid/liquid interface. Films will be formed when $\cos\theta = 1$, id. when $\lambda = -2\gamma$. This condition makes the average free energy of the molecules of the film less than that of the molecules in the bulk drop phase. The existence of a liquid drop over the substrate means that the bonds between the liquid molecules and the solid surface have decreased their strength.

Application of Eq. (9) to the static contact angle calculation (Table 1) of paraffin on Mo-contaminated surfaces and on Al_2O_3 ones makes it possible to make the following remarks. Despite the solid substrate, the advancing contact angles are always greater than the corresponding receding angles, because a thin layer of liquid paraffin can be formed on the solid surface after the solid slab has been introduced into the paraffin and then receded from it. Indeed in such a case the strength of the bonds between two molecules of paraffin is always greater than the bonds between the molecules of paraffin and any solid 'clean' surface. In agreement with Eq. (8) the corresponding effective contact angle has to decrease. The cosine of the receding angle is equal to 1 for the Al_2O_3/paraffin systems, and is equal to 0.98 for the Mo-contaminated/paraffin interfaces. Thus, the nature of the liquid thin film formed between the metal-contaminated surface and the paraffin has a lower stability than that formed between the alumina surface and the paraffin. The experimental value of the paraffin surface tension turned out to be equal to 32×10^{-3} J m^{-2}. Using this value with the different contact angles, Eq. (8) leads to the average partial free energy of the molecules of the solid/liquid interfaces for the different situations (see Table 1, last columns). For the Mo-contaminated/paraffin system this parameter is equal to $-60.9\times10^{-3}\pm10^{-2}$ J m^{-2} when the Mo-contaminated slab is introduced into the paraffin and it is equal to $-63.3\times10^{-3}\pm10^{-2}$ J m^{-2} when the Mo-contaminated slab is taken out from the liquid phase. By comparison with the same experimental situation the Al_2O_3/paraffin system yields to $-62.6\times10^{-3}\pm10^{-2}$ J m^{-2} and $-64.0\times10^{-3}\pm10^{-2}$ Jm^{-2}. If the average potential λ and the surface tension γ are the parameters that govern the equilibrium shape of a liquid drop over a substrate, the thermodynamic driving force that rules any movement of the drop on the surface should be described in terms of differential decreases of these integral and partial free energies. When two equal drops of paraffin are placed on two different substrates in a non-equilibrium state, they will tend to an equilibrium state. The lower the average partial free energy λ, the greater will be the change in the free energy, that will drive the system to the final solid/liquid equilibrium configuration. Thus, if the kinetic terms concerning the dynamics of the paraffin on the two substrates are comparable, the tendency of a liquid paraffin to spread over a solid substrate would be enhanced by high strength bonds between the liquid phase and the substrate. The above reported calculation suggests this possibility, while the measured paraffin spreading data are an indirect confirmation of this inference. When viscous flow mechanisms are associated with the spreading step also the surface viscosity of the liquid paraffin should be decreased by the existence of low negative values of λ, because the strong bonding of the paraffin to the substrate can make a paraffin film more stable than a paraffin liquid drop. The difference in the diffusion coefficient values concerning the Mo-contaminated/paraffin system and the alumina/paraffin one are consistent with these observa-

tions when they are compared with the corresponding differences in λ. Following this line of argument the experimental data reported in this paper also illustrate that the lower the calculated average interface partial free energy λ, the lower is the bulk viscosity and the intrinsic viscosity of the suspensions. On these grounds it seems reasonable to conclude that to control the bulk rheological behavior of 10 μm sized Mo and Al_2O_3 particles dispersed in liquid paraffin, it is important to control the interfacial solid/liquid forces as they happen in the colloidal ceramic processing.[9]

As an example of this possibility let us consider a different type of alumina formed by a set of particles averaging around 15 μm in size mixed with <1 μm grains of the same chemical composition (see Fig. 13). When these particles are dispersed in paraffin the contribution of the interfacial solid/liquid energy is higher than that concerning the 10 μm particles dispersed in paraffin at the same volume fraction, because the value of the interfacial solid–liquid area is increased. The prediction, based upon the findings and model discussed above, is that the value of the viscosity of the new alumina suspension should increase with respect to the value obtained with alumina suspension at the same volume fraction where the interfacial terms play a minor role. Fig. 14 (compare the slopes of curves b and d) proves that this is the case. Furthermore, since a lowering of the interfacial partial energy level corresponds to an increase in the global interfacial forces between the particles, the new suspension can be characterized also by significant yield stress τ_0. The data reported in Fig. 14 (see curve d) are consistent with this interpretation.

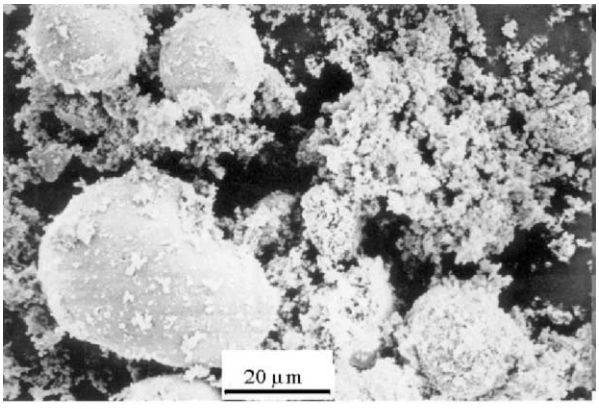

Fig. 13. Typical SEM picture of II–Al_3O_3 powder (1000×).

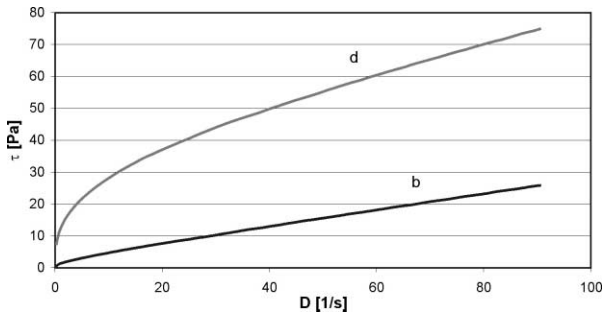

Fig. 14. Typical flow behavior for alumina/paraffin system: (b) 10% I–Al_3O_3 suspension; (d) 10% II–Al_3O_3 suspension; maximum applied shear rate $D = 100\ s^{-1}$.

5. Conclusions

1. Powders of contaminated molybdenum in the 10 μm range size dispersed in liquid paraffin at 20 °C obey the Newton law, equivalent interfacial solid/liquid area of alumina/paraffin suspension obey a flow behavior described by the Herschel–Bulkley model.
2. The dependence of viscosity on the volume fraction of the dispersed solid phase has been proved to fit the Einstein equation for molybdenum system, and the Krieger–Dougherty relationship for the alumina system.
3. Spreading of liquid paraffin at 20 °C and dynamic contact angle measurements on molybdenum contaminated surface and on alumina one show that the interaction between the molybdenum contaminated surface and liquid paraffin are stronger than those arising in the alumina/paraffin system.
4. The evidence that the intrinsic viscosity of the molybdenum contaminated suspension is greater than the intrinsic viscosity of the alumina one can be related to the evidence that the interaction between the Mo-contaminated surfaces and paraffin are greater than the same interaction between the alumina/paraffin system.

Acknowledgements

Conversations and discussions with Professor A. W. Searcy and Miguel Salmeron were very helpful to accomplish this work. We are indebted to Mr. S. Cerchi and to A. Tagnin for technical support in the early stage of this research. The research has been sponsored by the Nationwide CNR Project: MSTA II (*Progetto Finalizzato Materiali Speciali per Tecnologie Avanzate II*) contract number 9901739.PF.34 and partially under the sponsorship of the University of Genoa.

References

1. Collin, M. and Rowcliffe, D., Analysis and prediction of thermal shock in brittle materials. *Acta Mater.*, 2000, **48**, 1655–1665.

2. Mataga, P. A., Deformation of crack-bridging ductile reinforcements in toughened brittle materials. *Acta Metall.*, 1989, **37**, 3349–3359.
3. Sbaizero, O., Acts from the IV AIMAT Nat. Congr. Ed PTM 1998, pp. 59–67.
4. Wang, S. C. and Wei, W. C. J., Characterization of Al_2O_3 composites with Mo particulates. *Nano Structured Materials*, 1998, **42**, 983–1000.
5. Pezzotti, G., Suenobu, H., Nishida, T. and Sbaizero, O., Measurement of microscopic bridging stresses in an alumina molybdenum composite by in-situ fluorescence spectroscopy. *J. Am. Ceram. Soc.*, 1999, **82**, 1257–1262.
6. C.N.R. Italy Nation Wide Project M.R.S.T.II Ceramic Materials, 1999.
7. Ferrari A., *Preparazione di Miscele di Allumina e Molibdeno Tramite Dispersione delle Polveri in Fasi Liquide Paraffiniche*. Thesis. Faculty of Engineering, University of Genoa, 2001.
8. Edwards, D. A., Brenner, H. and Wasan, D. T., *Interfacial Transport Process and Rheology*. Butterworth-Heinemann, Boston, 1991.
9. Lewis, J. A., Colloidal processing of ceramics. *J. Am. Ceram. Soc.*, 2000, **83**, 2341–2359.
10. Velamakanni, B. V., Chang, J. C., Lange, F. F. and Pearson, D. S., New method for efficient colloidal particle packing via modulation of repulsive lubricating hydration forces. *Langmuir*, 1990, **6**, 1323–1325.
11. Lange F. F., New interparticle potential paradigm for advanced powder processing; In *Ceramic Powder Science IV*, 185–201, ed. Hirano, Messling and Hausner. American Ceramic Society, Westerville OH.
12. Weast, R. C. and Astle, M. J., *CRC Handbook of Chemistry and Physics*, 72nd edn.. CRC Press inc, Boca Raton, FL, 1992.
13. Israelachvili, J., *Intermolecular and Surface Forces*, II edn. Academic Press Inc, London, 1980.
14. Adamson, A. W. and Gast, A. P., *Physical Chemistry of Surfaces*. Wiley Interscience, New York, 1997.
15. Wang, L., Sigmund, W. and Aldinger, F., Systematic approach for dispersion of silicon nitride powder in organic media (I–II). *J. Am. Ceram. Soc.*, 2000, **83**, 691–702.
16. Xu. L. and Salmeron, M., Studies of wetting and capillary phenomena at nanometer scale with scanning polarization force microscopy. In *Nano-Surface Chemistry*. Rosoff-Dekker Inc., 1989.
17. Schwartz, A. M. and Perry, J. W., *Surface Active Agent*. Interscience Publishers Inc, New York, 1949.
18. Della Volpe, C., Dirè, S. and Pagani, E., A comparative analysis of surface and surface tension of hybrid silica films. *J. Non-Crystalline Solids*, 1997, **209**, 51–60.
19. Astarita, G., Mannucci, G. and Nicolais, L., *Rheology*. Plenum Publishing Corporation, New York, 1980 pp. 209–225.
20. Struble, L. and Sun, G. K., Viscosity of portland cement paste as a function of concentration. *Adv. Cem. Based Mat.*, 1995, **2**, 62–69.
21. Krieger, I. M., Rheology of monodispersed latices. *Adv. Colloid Interface Science*, 1972, **3**, 111.
22. Landau, L. and Lifshitz, E., *Mecanique des Fluides*. MIR Moskow, 1972, pp. 98, 99.
23. Hauffe K., Corrosion of metals in gases and aqueous solutions. In Reactivity of Solids, Mitchell, DeVries, Roberts, Cannon. ed. Wiley Interscience, New York.
24. Searcy, A. W., The dependence of particle shapes on partial free energies of bonding to inert substrates. *Scripta Mater.*, 1999, **8**, 979–982.